SUPPLEMENTAL DATA

Materials

Each cell line was originally purchased from ATCC. Cell culture media such as Eagle's Minimum Essential Medium (EMEM), Dulbeco's Modified Eagle's Medium (DMEM) and Roswell Park Memorial Institute medium 1640 (RPMI-1640) were purchased from GIBCO. All other cell culture reagents such as fetal bovine serum (FBS), penicillin-streptomycin, and 2 mM glutamine were purchased from Life Technologies. Amine-coated 24-well cultureware plates were obtained from BD Biosciences (San Jose, CA). Accutase was acquired from BioLegend (San Diego, CA). Human FAP APC-conjugated (Catalog No. FAB3715A-100) and murine FAP monoclonal rat IgG (Catalog No. MAB9727-SP) antibodies were procured from R&D Systems (Minneapolis, MN). Common cell culture materials such as culture flasks and syringes were purchased from VWR (Chicago, IL). Fluorescence based assays were measured with a BioTek Synergy Neo2 plate reader. Flow cytometry was analyzed using an Attune NxT Acoustic Focusing Flow Cytometer**.** LRMS-LC/MS was performed with an Agilent 1220 Infinity LC with a reverse-phase XBridge Shield RP18 column (3.0 x 50 mm, 3.5 µm). Radiolabeling was achieved using a Fisherbrand Isotemp Digital Dry Bath/Block Heater (Waltham, MA). Radio-HPLC analysis was performed with an Agilent 1260 Infinity II equipped with a Flow-RAM detector purchased from LabLogic (Brandon, FL) and a reverse-phase XBridge Shield RP18 column (3.0 x 50 mm, 3.5 µm). SPECT/CT scans were acquired with a VECTor/CT system with a clustered multi-pinhole high-energy collimator (MILabs, Utrecht, The Netherlands). Radioactive binding and biodistribution studies were measured with a Packard Cobra Gamma Counter (Niederösterreich, Austria).

Synthesis

4-methyl isoindoline-4-carboxylate hydrochloride was purchased from PharmaBlock (Hatfield, PA). Boc-L-pyroglutamic acid benzyl ester was purchased from Accela ChemBio (San Diego, CA). 4-(*p*-iodophenyl)butyric acid was purchased from AstaTech, Inc (Bristol, PA). NHS-ester-PEG_6-NHFmoc and Propargyl-PEG_6-amine were purchased from BroadPharm. DOTA-NHS ester was purchased from Macrocyclics. Lysine was purchased from AAPPTec (Louisville, KY). Fmoc-L-Lys-OtBu hydrochloride, 4,4-Difluoro-L-prolinamide hydrochloride, and HATU were purchased from Chem-Impex International (Chicago,

IL). 4-Ethynylbenzoic acid and mono-Fmoc ethylene diamine hydrochloride were purchased from AA Blocks LLC (San Diego, CA). Di-tert-butyl dicarbonate was purchased from Oakwood Chemical (Estill, SC). Palladium, 10% on carbon, was purchased from Alfa Aesar (Haverhill, MA). Sodium borohydride, N-bromosuccinimide, triphenylphosphine, sodium azide, lithium bis(trimethylsilyl)amide, tert-butyl-bromoacetate, 1,8-diazabicyclo[5.4.0]undec7-ene, pyridine, imidazole, phosphoryl chloride, diethyl either, DIPEA, TFA, THF, DMF, DCM, MeOH, DMSO, and all other reagents were purchased from Sigma-Aldrich (St. Louis, MO). All synthesized molecules were purified using either flash chromatography (CombiFlash RF, Teledyne) or RP-HPLC (Agilent 1200 Instrument) with an XBridge OBD preparative column (19 x 150 mm, 5 μm) purchased from Waters (Milford, MA).

Analyses of FAP Expression by Single Cell RNA-seq

We exploited scRNA-seq data published by Qian et al (*1*) that profiled the transcriptomes of more than 233,000 single cells from 34 cancer patients. For our purposes, FAP overexpression data on tumor cells collected from fourteen breast cancer patients (44,026 cells), five ovarian cancer patients (45,115 cells), seven colorectal cancer patients (41,758 cells), and eight lung cancer patients (88,668 total cells) from the VIB KU Leuven Center for Cancer Biology database were analyzed by following SCope tutorials (*2*). All cell types were selected using the lasso tool and the corresponding metadata were downloaded and analyzed. A FAP expression level = 0 was considered FAP-negative, while a FAP expression level > 0 was considered FAP-positive.

Cell Culture and Sorting

Cell cultures were maintained in DMEM (HEK and Hs894 cells), EMEM (HT1080 and U87MG cells) or RPMI-1640 supplemented with 1% 2 mM glutamine (4T1 and KB cells) at 37°C in a 5% CO_2 and 95% humidified atmosphere. 10% FBS and 1% penicillin-streptomycin were added to all media. Generation, characterization, and culture of HT1080-hFAP cells were previously reported (*3*). Regular screening for mycoplasma contamination was performed to ensure integrity of all studies, and contaminated cultures were discarded. HEK-hFAP cells with high levels of FAP expression were isolated by cell sorting using an anti-human FAP monoclonal antibody and a BD LSRFortessa Flow Cytometer. The high FAP expressing cells were cultured and stored for subsequent confocal and binding studies.

Radiosynthesis and Formulation

Stock solutions of FAP6 conjugates were diluted in ammonium acetate (0.5 M, pH 8.0) to 0.5 mM. Radio-HPLC method = (A) 20 mM ammonium bicarbonate buffer (pH 7) and (B) acetonitrile in a linear gradient from 5% B to 95% B over 15 minutes. After confirmation of successful radiolabeling by radio-HPLC analysis (radiopurity > 95%, radiochemical yield > 90%), sodium-diethylenetriamine pentaacetate (DTPA-Na) solution (5 mM, pH 7.0) was added at a final concentration of 0.2 mM to complex any unreacted traces of radioactive isotope. Conjugates were formulated in 5% ethanol in PBS (v/v) containing 10% sodium ascorbate (w/v) and 0.5% L-methionine (w/v) for all *in vitro* and *in vivo* studies.

Whole-Cell Assays

Flow Cytometry. Samples containing ~100,000 cells were suspended in staining buffer (2% FBS in PBS) and incubated for 20 minutes on ice with FAP antibodies (1:100 dilution), then washed with fresh solution three times. Murine cell lines were further stained with an APC-conjugated secondary antibody and washed in similar fashion. Cells were then resuspended in staining buffer for flow cytometry analysis. Singlet cells were gated via FSC and SSC examination, and FAP-positive subpopulations were established by non-staining controls on the RL1 channel. Final figures were generated using FlowJo (version 10.8) software.

Displacement Assay. 250,000 HEK-hFAP cells were seeded per well into amine-coated 24-well plates and allowed to reach confluence before they were incubated with 10 nM FAP6-rhodamine (*3*) in the presence of increasing concentrations of FAP6-DOTA or FAP6-IP-DOTA. After incubation for one hour at 4°C, the cells were washed three times with PBS to remove unbound fluorescence and dissolved in 1% SDS. The samples were then transferred to 96-well, clear bottom, black wall plates and cell-bound fluorescence was measured with a BioTek Synergy Neo2 plate reader. Wavelengths were set to λ_{ex} = 552 nm and λ_{em} = 575 nm and cell-bound fluorescence was plotted against the logarithm of the concentrations of the FAP6 conjugates in nM. A K_d of 2.67 nM for FAP6-rhodamine was used to calculate the K_i of the FAP6 conjugates using one-site binding nonlinear fit. All samples were performed in triplicate.

Direct Binding. 100,000 Hs894 CAFs were seeded in 24-well plates and allowed to grow to confluence prior to the addition of either ^{111}In-FAP6-DOTA or ^{111}In-FAP6-IP-DOTA in the absence or presence of excess FAP6 ligand (to competitively block radioactive binding). After incubation for 1h at room temperature, the cells were washed three times with PBS to remove unbound radioactivity and dissolved in 1.0 M NaOH. The samples were then transferred to tubes and cell-bound radioactivity was measured

using a gamma counter. A specific binding constant was calculated using one-site specific binding nonlinear regression after subtracting competition counts from total binding counts. All samples were performed in triplicate.

Internalization. 200,000 HT1080-hFAP cells were seeded into each well of 24-well plates and grown to confluence. The media was removed, and 25 nM of ^{111}In-FAP6-DOTA or ^{111}In-FAP6-IP-DOTA in 0.25 mL of media containing 1% FBS was added to all wells. The plates were incubated at 37ºC for the indicated times, after which the media was removed, and the wells were washed three times with PBS to remove unbound radioactivity. To determine the total radioactivity absorbed by the cell, a subset of samples was immediately lysed with 1.0 M NaOH. Additional samples were incubated for 1 minute with HEPES buffer (pH 2.5) to remove surface-bound radioactivity, after which the cells were dissolved with 1.0 M NaOH to harvest the internalized radioactivity. All samples were transferred to tubes for gamma counter measurements, and internalized radioactivity was normalized as a percent of total absorbed radioactivity by the cells. All samples were performed in triplicate.

Radiosensitivity. 100,000 4T1, HT29, KB, or U87MG cells were seeded into 12 well plates and then promptly irradiated while still suspended (i.e., before the cells adhered to the bottom of the wells). Doses of 2, 4, 8, 12, and 20 Gy were administered with a photon beam from a 6MV Linac (Varian EX). A 1.5 cm bolus was placed underneath the plates for full electron equilibrium. Confluency of the cells were visually estimated every other day to gauge relative radiosensitivities of the difference cell lines. All samples were performed in triplicate.

Animals

6-week-old (16-19 g) female Balb/c mice were purchased from Charles River. 12-week-old female athymic nu/nu mice (23-27 g) were purchased from Envigo. Up to 5 mice were housed in a single cage with corn cob bedding and paper strips for enrichment. Temperatures and humidity were maintained at 21–22°C and 30–70%, respectively, throughout all studies. Prior to initiation of studies, mice were housed in cages on ventilated racks with filtered air, which were changed biweekly. Upon initiation of studies, mice were housed in static cages, which were changed weekly. All tumor cells (4T1, KB, HT29, and U87MG) were suspended in PBS at time of inoculation in appropriate mouse breeds. Nu/nu mice were inoculated on their shoulder with 5 x 10^6 cells of HT1080-FAP cells for specificity studies.

SPECT/CT Scans

Tumors were allowed to grow up to ~1 cm^3 before initiating SPECT/CT studies. Mice were injected intravenously via the lateral tail vein with 1-30 nmol of FAP6-DOTA or FAP6-IP-DOTA radiolabeled with ^{111}In (~10 MBq) or ^{177}Lu (~55 MBq) in 100 µL of vehicle. FAP6 conjugates were radiolabeled at a specific activity of ~2 MBq/nmol for ^{111}In or ~11 MBq/nmol for ^{177}Lu, unless indicated otherwise. Immediately prior to initiation of the scans, mice were anesthetized by inhalation of ~3% isoflurane using a 1.25 L/min flow rate of oxygen and maintained at these conditions on top of a heating strip to regulate murine body temperatures in the prone position without additional fixation for the duration of the scan. The SPECT scans were acquired with a 0.35 mm pinhole (mouse whole body) collimator, 15–60 second acquisitions per bed position across ~50 bed positions, totaling 20–60 minutes per mouse. The CT scans were acquired with an X-ray source set at 60 kV and 615 µA. The SPECT images were reconstructed with U-SPECT II software using ^{111}In γ-energy windows of 171 and 241 keV or ^{177}Lu γ-energy window of 208 keV. A POS-EM algorithm was used with 16 subsets and 4 iterations on a 0.8 mm voxel grid. A 3.0 median filter was applied to all scans. Background remover was only applied to remove low levels of noise observed outside the bodies of the mice. Bladders were masked as needed within the first 24 hours to enable visualization of the biodistribution of the FAP6-targeted radiotracers.

Radioactive Biodistribution

4T1 tumors were allowed to grow to ~250–500 mm^3 before initiating biodistribution studies. Each tumor-bearing mouse was intravenously injected via the lateral tail vein with 5 nmol of FAP6-DOTA radiolabeled with ^{177}Lu (~3.7 MBq) or 5 nmol of FAP6-IP-DOTA radiolabeled with ^{111}In (~0.37 MBq) or ^{177}Lu (~3.7 MBq) in 100 µL of vehicle. Mice were euthanized by CO_2 asphyxiation at 1, 4, 24, 72, or 120 hours post injection. Organs were thoroughly washed with buffer to remove excess blood before gamma counter analysis. Results were decay corrected then normalized as percentages of the injected dose per gram of tissue (%ID /g) and provided as mean ± standard error.

Dosimetry Calculations

All absorbed doses were calculated with OLINDA 2.2.3 software using the *ex vivo* biodistribution data from Fig. 4B and 4D. Estimates for healthy organs were calculated assuming a 25 g mouse phantom. Tumor dose estimates were calculated with the sphere model. Time-activity curves were fitted to the biodistribution data of each organ individually with exponential functions. Estimates for healthy organs were calculated assuming a 25 g mouse phantom.

Radiotherapy

4T1, HT29, KB, and U87MG tumors were grown to ~109 mm^3 (n = 5 per group), ~169 mm^3 (n = 4 per group), ~52 mm^3 (n = 5 per group), or ~173 mm^3 (n = 5 per group), respectively, then randomly divided into control and treatment groups. Each tumor-bearing mouse was intravenously injected via the lateral tail vein with up to 5 nmol of FAP6 conjugates radiolabeled with ^{177}Lu (≤ 55 MBq) in 100 μL of vehicle. Specific activities of 1.8 MBq/nmol were tested in HT29, U87MG, and 4T1 tumor-bearing mice; 3.6 MBq/nmol in U87MG, KB, and 4T1 tumor-bearing mice; 11 MBq/nmol in 4T1 tumor-bearing mice. Radioactive injections of 55 MBq were accompanied with an injection of amino acid solution (30 mg of lysine in PBS) into the intraperitoneal cavity. Furthermore, 4T1-tumor bearing mice injected with 55 MBq of ^{177}Lu-FAP6-IP-DOTA were measured every other day by two separate people in blinded fashion (i.e., they did not know which mice were control vs. treated). Tumor volumes were calculated as $0.5 \times L \times W^2$, where L is the longest axis (in millimeters), and W is the axis perpendicular to L (in millimeters). Humane endpoint criteria were defined as weight loss of more than 20% of the initial body weight, a tumor volume of more than 1,800 mm^3 for human xenografts or 1,500 mm^3 for syngeneic murine cancers, or open ulceration.

Pathology & Histology

Mice were randomly selected from control and treatment groups (as indicated) for further evaluation at the conclusion of the radiotherapy studies. Myocardium, liver, and kidneys were harvested, washed, fixed in a 10% formalin solution for 48-72 hours. Organs were then maintained in a 70% ethanol solution until radioactivity had fully decayed, after which they were submitted to the Histology Research Laboratory at Purdue University to be embedded in paraffin, sectioned, and stained with hematoxylin and eosin (H&E). Additional tumor samples were stained with a FAP antibody (1:150 dilution) for histopathological analysis.

Statistical Significance

Statistical significance in tumor sizes was analyzed by unpaired two-tailed t test (*$P < 0.05$, **$P < 0.01$, ***$P < 0.001$). Statistical significance of survival rates was determined by Log-rank (Mantel-Cox) test (*$P < 0.05$).

Synthesis of FAP6 Conjugates

Synthesis of key FAP6 intermediates **4** and **9** were performed as reported previously (*3,4*).

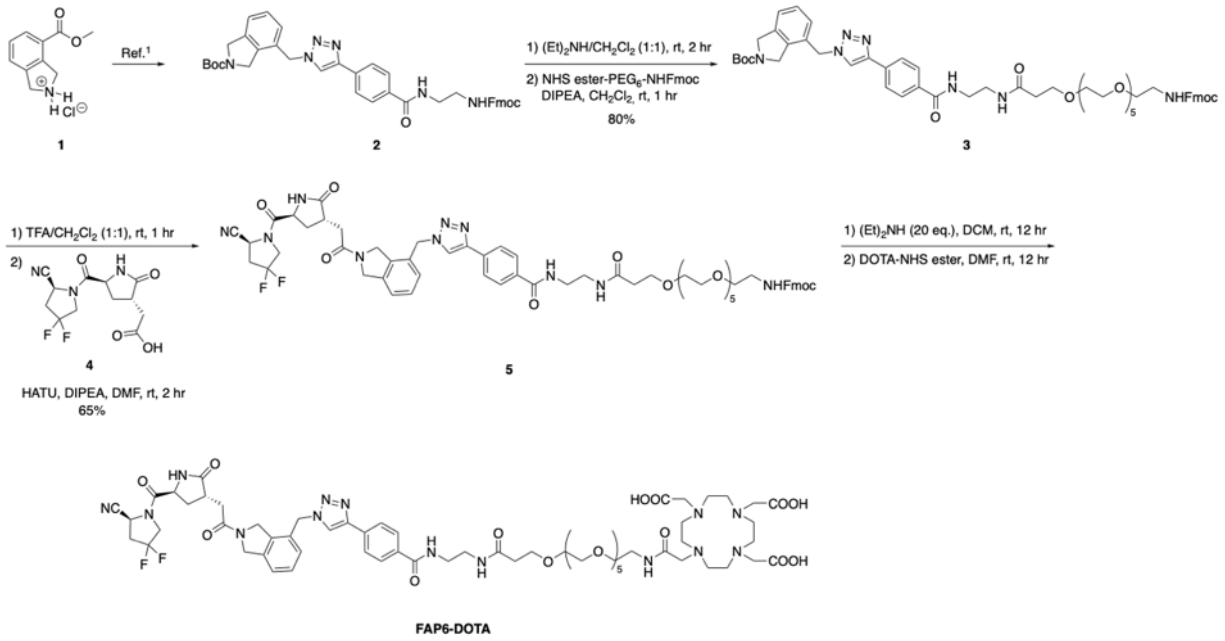

Supplemental Scheme 1. Synthesis of FAP6-DOTA.

Synthesis of tert-butyl 4-((4-(4-((1-(9H-fluoren-9-yl)-3,25-dioxo-2,7,10,13,16,19,22-heptaoxa-4,26-diazaoctacosan-28-yl)carbamoyl)phenyl)-1H-1,2,3-triazol-1-yl)methyl)isoindoline-2-carboxylate (3): Compound **2** (400mg, 0.584 mmol) was dissolved in a DCM:MeOH solution (1.0 + 0.5 mL), then $(Et)_2NH$ (1.0 mL) was added before stirring at room temperature for 2 hours. The reaction mixture was evaporated under reduced pressure and the resulting crude residue purified by flash chromatography using a DCM:MeOH mobile phase. The resulting free amine of compound **2** was dissolved in DCM (1 mL for 1 mmol) followed by NHFmoc-PEG_6-NHS ester (1.2 eq) and DIPEA (2.0 eq), and the resulting solution was stirred under inert atmosphere at room temperature for 2 hours. The reaction mixture was evaporated under reduced pressure and the resulting crude residue was purified by flash chromatography using a DCM:MeOH mobile phase to provide the compound **3** as white solid. LC/MS for **3**: LC/MS (m/z): calculated $[M+H]^+$ for $C_{55}H_{69}N_7O_{12}$: 1021.2, observed: 1021.2g/mol.

Synthesis of (9H-fluoren-9-yl)methyl (1-(4-(1-((2-(2-((3S)-5-((S)-2-cyano-4,4-difluoropyrrolidine-1-carbonyl)-2-oxopyrrolidin-3-yl)acetyl)isoindolin-4-yl)methyl)-1H-1,2,3-triazol-4-yl)phenyl)-1,6-dioxo-9,12,15,18,21,24-hexaoxa-2,5-diazahexacosan-26-yl)carbamate (5):

Compound **3** (250 mg, 0.268 mmol) was dissolved in DCM (1.0 mL) at room temperature, then TFA (0.5 mL) was added and stirred for 30 minutes. The reaction mixture was evaporated and dried under vacuum. In a separate round bottom flask the carboxylic acid-bearing compound **4** (*3*) (100 mg, 0.333 mmol) was dissolved in DMF (0.5 mL) with HATU (151 mg, 0.399 mmol), DIPEA (0.170 mL, 0.999mmol) and the reaction mixture stirred was stirred under inert atmosphere at room temperature for 10 minutes. The amine generated *in situ* from compound **3** (220 mg, 0.268 mmol) was dissolved in DMF (1 mL), added to the above reaction mixture, and stirred for 2 hours. The reaction mixture was diluted with water (15 mL) and stirred at room temperature for 15 min, after which the formed black turbidity formed was filtered then redissolved in a DCM:MeOH solution. After evaporation of the organic layer, the obtained crude residue was purified by reverse phase preparative high performance liquid chromatography (HPLC) (A= 20 mm NH_4OAc buffer (pH = 7), B = CH_3CN, solvent gradients 5% B to 95% in 60 min provided the compound **5** as white solid. LC/MS for **5**: LC/MS (m/z): calculated $[M+H]^+$ for $C_{62}H_{72}F_2N_{10}O_{13}$: 1204.3, observed: 1204.3 g/mol.

Synthesis of 2,2',2''-(10-(1-(4-(1-((2-(2-((3S)-5-((S)-2-cyano-4,4-difluoropyrrolidine-1-carbonyl)-2-oxopyrrolidin-3-yl)acetyl)isoindolin-4-yl)methyl)-1H-1,2,3-triazol-4-yl)phenyl)-1,6,28-trioxo-9,12,15,18,21,24-hexaoxa-2,5,27-triazanonacosan-29-yl)-1,4,7,10-tetraazacyclododecane-1,4,7-triyl)triacetic acid (FAP6-DOTA):

Compound **5** (175 mg, 0.16 mmol) was dissolved in DCM (0.5 mL), then $(Et)_2NH$ (20 eq) was added and stirred at room temperature overnight. Reaction progress was monitored by LC/MS for complete deprotection of the Fmoc group to generate the free amine from **5:** LC/MS (m/z) calcd for: $C_{47}H_{63}F_2N_{10}O_{11}[M+H]$: 981.4 found: 981.4 g/mol. The reaction mixture was evaporated under reduced pressure and the obtained crude residue was triturated with EtOAc (2 x10 mL) then diethyl ether (3 x 10 mL), followed by filtration and dried under vacuum before further use. The free amine from compound **5** (0.03 mmol) and DOTA-NHS ester (0.045 mmol) were dissolved in anhydrous DMF (0.5 ml) was DIPEA was added (0.091 mmol) before stirring overnight. Reaction progress was monitored by LC/MS for complete

consumption of starting material, after which the reaction mixture was diluted with water (0.5 mL) and purified via RP-HPLC [A = 20 mM NH_4OAc buffer (pH 7.0) and B = CH_3CN, solvent gradient 5% B to 35% B in 60 minutes] to yield **FAP6-DOTA**. LC/MS for **FAP6-DOTA**: LC/MS (m/z): calculated $[M+H]^+$ for $C_{63}H_{88}F_2N_{14}O_{18}$: 1368.5, observed: 1368.5 g/mol.

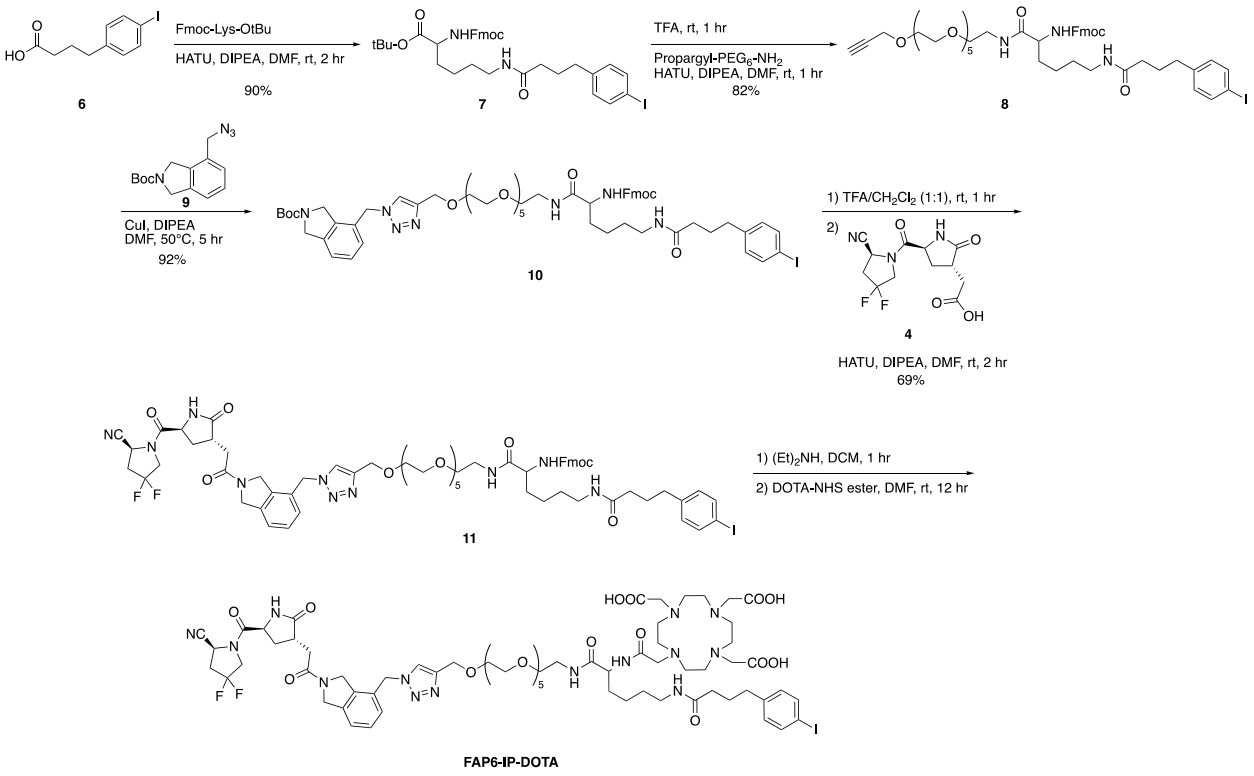

Supplemental Scheme 2. Synthesis of FAP6-IP-DOTA.

Synthesis of N2-(((9H-fluoren-9-yl)methoxy)carbonyl)-N6-(4-(4-iodophenyl)butanoyl)-L-lysine (7):

4-(*p*-iodophenyl)butyric acid (Compound **6**) (500 mg, 3.460 mmol) was dissolved in anhydrous DMF (10 mL) with HATU (1.3 g, 3.460 mmol) and anhydrous DIPEA (3 eq) then stirred for 10 minutes at room temperature under inert gas. Fmoc-Lys-OtBu HCl (1.6 g, 3.460 mmol) in anhydrous DMF (5.0 mL) and DIPEA (1.15 mL, 6.92 mmol) were added to the above reaction mixture. The resulting solution was stirred under inert atmosphere at room temperature for 2 hours as reaction progress was monitored by LC/MS. After complete consumption of the starting materials, the reaction mixture was diluted with water and extracted into EtOAc (2 x 50 mL). The combined organic layers were further washed with water (50 mL),

brine (50 mL) and dried over anhydrous magnesium sulphate. The crude product was obtained by filtration then evaporation under reduced pressure, and purified by flash chromatography using a Hex:EtOAc mobile phase to provide compound **7** as a fluffy white solid. LC/MS for **7**: LC/MS (m/z): calculated $[M+H]^+$ for $C_{31}H_{33}IN_2O_5$: 697.6, observed: 697.6 g/mol.

Synthesis of (9H-fluoren-9-yl)methyl (R)-(33-(4-iodophenyl)-23,30-dioxo-4,7,10,13,16,19-hexaoxa-22,29-diazatritriacont-1-yn-24-yl)carbamate (8):

Compound **7** (545 mg, 0.782 mmol) was dissolved in neat TFA and stirred for one hour. Progress of the reaction was monitored via LC/MS. LC/MS (m/z): $[M+H]^+$ calculated for $C_{31}H_{33}IN_2O_5$, 641.5; observed mass 641.5. The deprotected carboxylic acid product was isolated *en vacuo* and used without further purification, by redissolving in anhydrous DMF with HATU (1 350 mg, 0.937 mmol) and anhydrous DIPEA (0.26 mL, 1.562 mmol) for 10 minutes. Propargyl-PEG_6-amine (300 mg, 0.937 mmol) was dissolved in anhydrous DMF and DIPEA (0.13 mL, 0.781 mmol) and added to the above reaction mixture. The resulting solution was stirred under inert atmosphere at room temperature for 2 hours. The reaction mixture was diluted with water, extracted with EtOAc, and evaporated under reduced pressure. The crude product was purified by flash chromatography using a DCM:MeOH mobile phase to yield compound **8** as a gummy white solid. LC/MS for **8**: LC/MS (m/z): calculated $[M+H]^+$ for $C_{46}H_{60}IN_3O_{10}$: 942.9, observed: 942.9 g/mol.

Synthesis of tert-butyl (R)-4-((4-(1-(9H-fluoren-9-yl)-5-(4-(4-(4-iodophenyl)butanamido)butyl)-3,6-dioxo-2,10,13,16,19,22,25-heptaoxa-4,7-diazahexacosan-26-yl)-1H-1,2,3-triazol-1-yl)methyl)isoindoline-2-carboxylate (10).

To a mixture of azide **9** (*3*) (210 mg, 0.764 mmol) and alkyne **8** (600 mg, 0.636 mmol) in dry DMF (5 mL) was added CuI (0.5 eq) and DIPEA (2.0 eq). The reaction mixture was stirred under inert gas at 50°C and for 1 hour. After cooling to room temperature, the reaction mixture was isolated *en vacuo*, redissolved in DCM, and diluted with saturated aqueous ammonium chloride (20 mL). The product was then extracted with DCM (2 x 50 mL). The organic extracts were combined, washed with water and brine, then evaporated. The crude residue was purified by flash chromatography using a DCM:MeOH mobile phase to yield

compound **10** as a brown gummy solid. LC/MS for **10**: LC/MS (m/z): calculated $[M+H]^+$ for $C_{60}H_{78}IN_7O_{12}$: 1217.2, observed: 1217.2 g/mol.

Synthesis of (9H-fluoren-9-yl)methyl ((R)-1-(1-((2-(2-((3S,5S)-5-((R)-2-cyano-4,4-difluoropyrrolidine-1-carbonyl)-2-oxopyrrolidin-3-yl)acetyl)isoindolin-4-yl)methyl)-1H-1,2,3-triazol-4-yl)-31-(4-iodophenyl)-21,28-dioxo-2,5,8,11,14,17-hexaoxa-20,27-diazahentriacontan-22-yl)carbamate (11).

To a solution of compound **10** (500.0 mg, 0.411 mmol) in DCM (5.0 mL) at room temperature was added TFA (1.0 mL), which was stirred for 60 minutes. The reaction mixture was evaporated and dried under vacuum. In a separate round bottom flask, carboxylic acid **4** (*3*) (150.0 mg, 0.439 mmol) was dissolved in DMF (1.0 mL) followed by HATU (200.0 mg, 0.526 mmol) and DIPEA (0.18 mL), and the resulting mixture was stirred under inert gas at room temperature for 10 minutes. The amine *in situ* generated from **10** (458 mg, 0.41 mmol) was dissolved in DMF (1 mL) and added to the above reaction mixture. The resulting solution was stirred at room temperature for 2 hours, after which it was diluted with water (15 mL) and stirred at room temperature for 10 minutes. The black turbidity formed in the mixture was filtered, then redissolved in DCM:MeOH and evaporated. The crude residue was purified by reverse phase preparative high performance liquid chromatography (RP-HPLC) [A = 20 mM NH_4OAc buffer (pH 7.0), B = ACN, gradient 5% B to 95% in 60 minutes] or by flash chromatography using a DCM:MeOH mobile phase to provide the compound **11** as a brown solid. LC/MS for **11**: LC/MS (m/z): calculated $[M+H]^+$ for $C_{67}H_{81}IN_{10}O_{13}$: 1400.3, observed: 1400.3 g/mol.

Synthesis of 2,2',2''-(10-((R)-1-(1-((2-(2-((3S,5S)-5-((R)-2-cyano-4,4-difluoropyrrolidine-1-carbonyl)-2-oxopyrrolidin-3-yl)acetyl)isoindolin-4-yl)methyl)-1H-1,2,3-triazol-4-yl)-22-(4-(4-(4-iodophenyl)butanamido)butyl)-21,24-dioxo-2,5,8,11,14,17-hexaoxa-20,23-diazapentacosan-25-yl)-1,4,7,10-tetraazacyclododecane-1,4,7-triyl)triacetic acid (FAP6-IP-DOTA).

Compound **11** (400 mg, 0.286 mmol) was dissolved in anhydrous DCM (0.5 mL) and diethylamine $(Et)_2NH$ (0.592 mL, 5.72 mmol) then stirred for overnight. Progress of the reaction was monitored via LC/MS. LC/MS (m/z): calculated $[M+H]^+$ for $C_{52}H_{71}F_2IN_{10}O_{10}$, 1178.1; observed: 1178 g/mol. Upon completion of the deprotection, the product was isolated via rotary evaporation, was triturated with EtOAc (2 x10 mL) then

diethyl ether (3 x 10 mL), followed by filtration and dried under vacuum before further use. The deprotected product was dissolved in anhydrous DMF (0.5 mL) and DIPEA (0.150 mL, 0.858 mmol) with DOTA-NHS ester (261 mg, 0.343 mmol) and stirred under inert atmosphere at room temperature for 12 hours. The crude product was purified via RP-HPLC [A = 20 mM NH_4OAc buffer (pH 5.0) and B = CH_3CN, solvent gradient 5% B to 35% B in 60 minutes] to yield **FAP6-IP-DOTA**. LC/MS for **FAP6-IP-DOTA**: LC/MS (m/z): calculated $[M+H]^+$ for $C_{68}H_{97}F_2IN_{14}O_{18}$, 1563.4, observed 1563.4 g/mol.

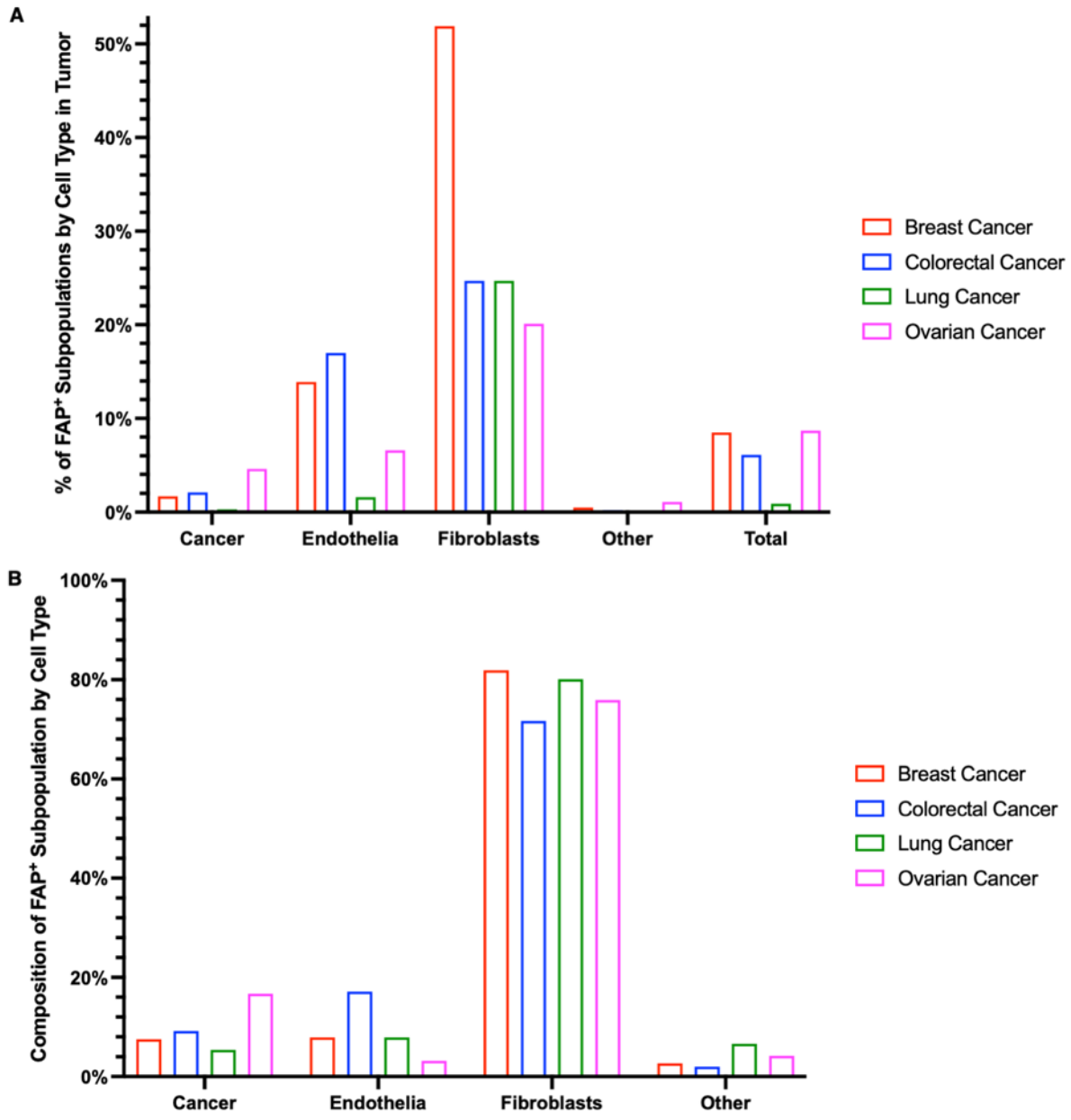

SUPPLEMENTAL FIGURE 1. (**A**) Quantification of the subpopulation within each major cell type that overexpresses FAP RNA in the indicated types of human solid tumors. Approximately 2.5% of all cancer cells vs. 30% of all fibroblasts upregulate FAP gene expression in human breast, colorectal, lung and ovarian tumors. (**B**) Identity analysis and relative quantification of the cells within the FAP-overexpressing subpopulation for each type of solid tumor, e.g., a cancer, endothelial or fibroblast cell type. For example, 9.7% of all FAP-overexpressing cells in the indicated solid tumors are cancer cells while 77.4% are fibroblasts. The "Other" category includes myeloid cells, T-cells, B-cells, dendritic cells, and mast cells.

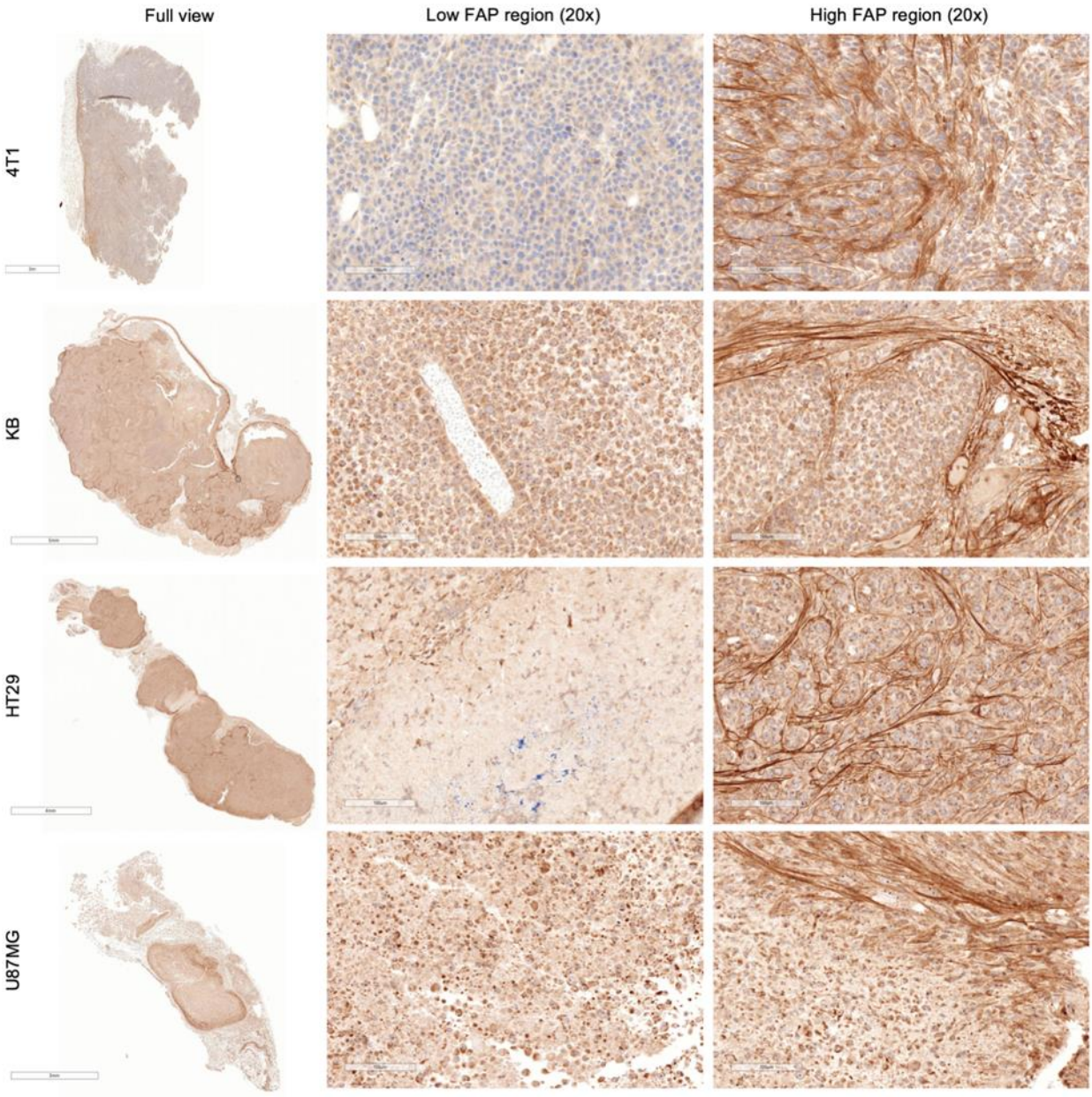

SUPPLEMENTAL FIGURE 2. FAP IHC stains of 4T1, KB, HT29, and U87MG tumors. Representative sections of FAP low and high regions within the tumor are also provided at 20x magnification.

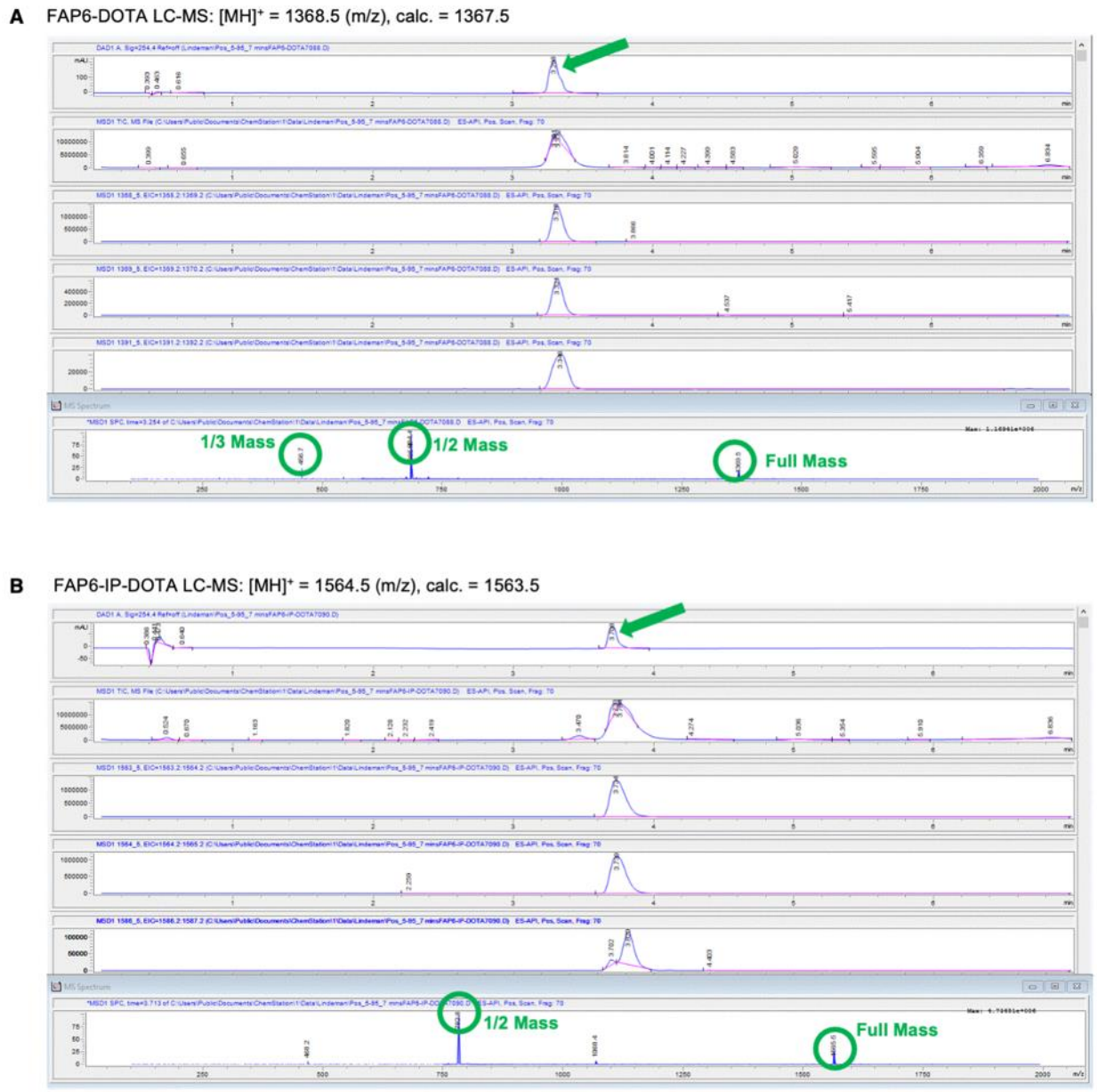

SUPPLEMENTAL FIGURE 3. LC/MS characterization of (**A**) FAP6-DOTA, and (**B**) FAP6-IP-DOTA. LC/MS conditions: gradient = 0.5 min 5% B → 4.5 min 95% B → 5.5 min 95% B → 6.0 min 5% B → 7.0 min 5% B [A = 20 mM pH 7 NH_4HCO_3, B = ACN]; flow rate = 0.75 mL/min; DAD = 190–900 nm sweep (λ = 254 nm extracted); ionization energy = 70 eV.

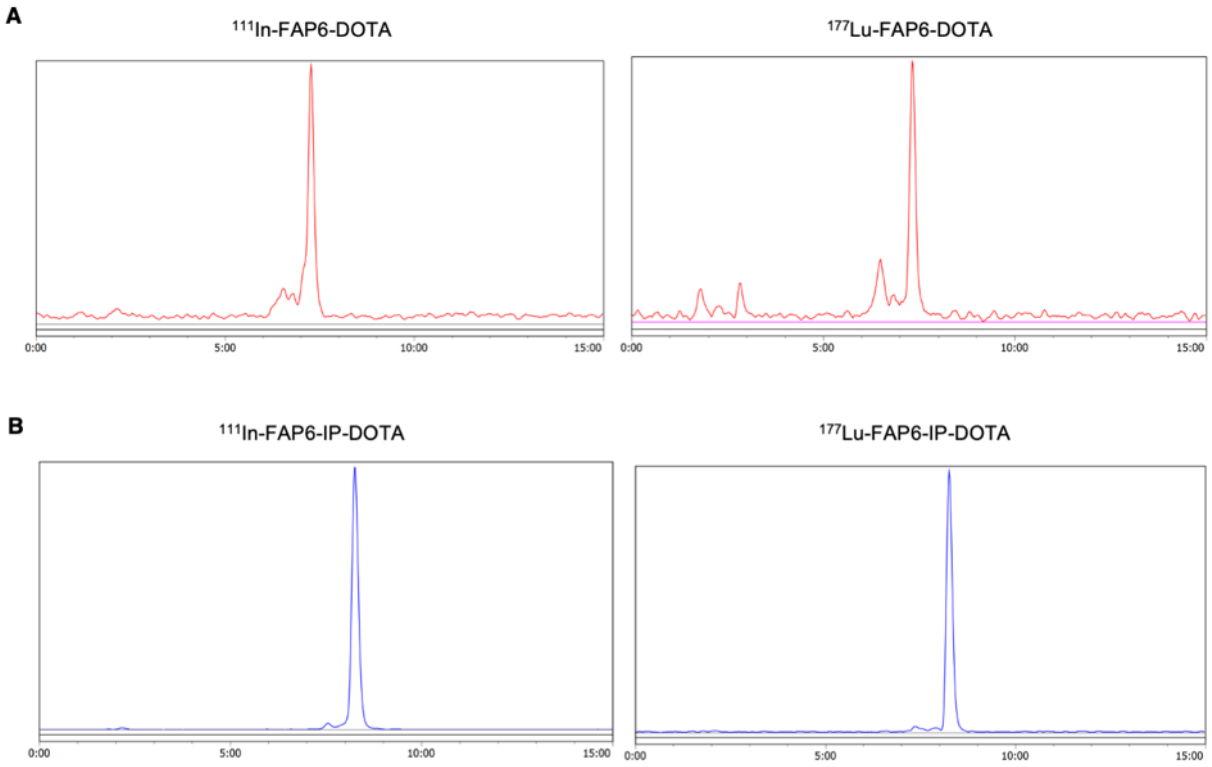

SUPPLEMENTAL FIGURE 4. Radiochromatograms of (**A**) ^{111}In-FAP6-DOTA and ^{177}Lu-FAP6-DOTA; (**B**) ^{111}In-FAP6-IP-DOTA and ^{177}Lu-FAP6-IP-DOTA. Radio-HPLC conditions: gradient = 0.5 min 5% B → 4.5 min 95% B → 10.0 min 95% B → 11.0 min 5% B → 14.0 min 5% B → 15.0 min 5% B [A = 20 mM pH 7 NH_4HCO_3, B = ACN]; flow rate = 0.75 mL/min; λ = 254 nm extracted.

A

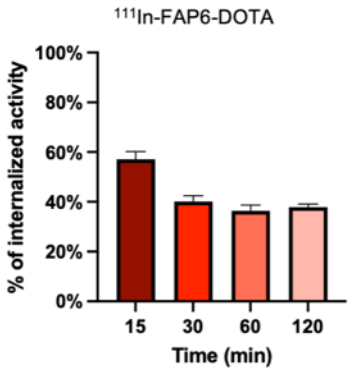

B

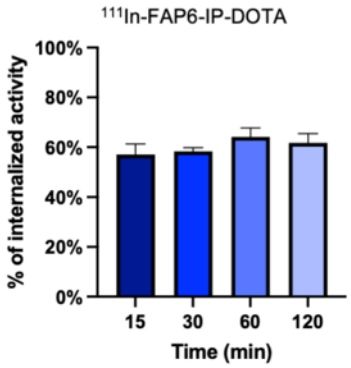

SUPPLEMENTAL FIGURE 5. Internalization of (**A**) ^{111}In-FAP6-DOTA or (**B**) ^{111}In-FAP6-IP-DOTA in HT1080-hFAP cells.

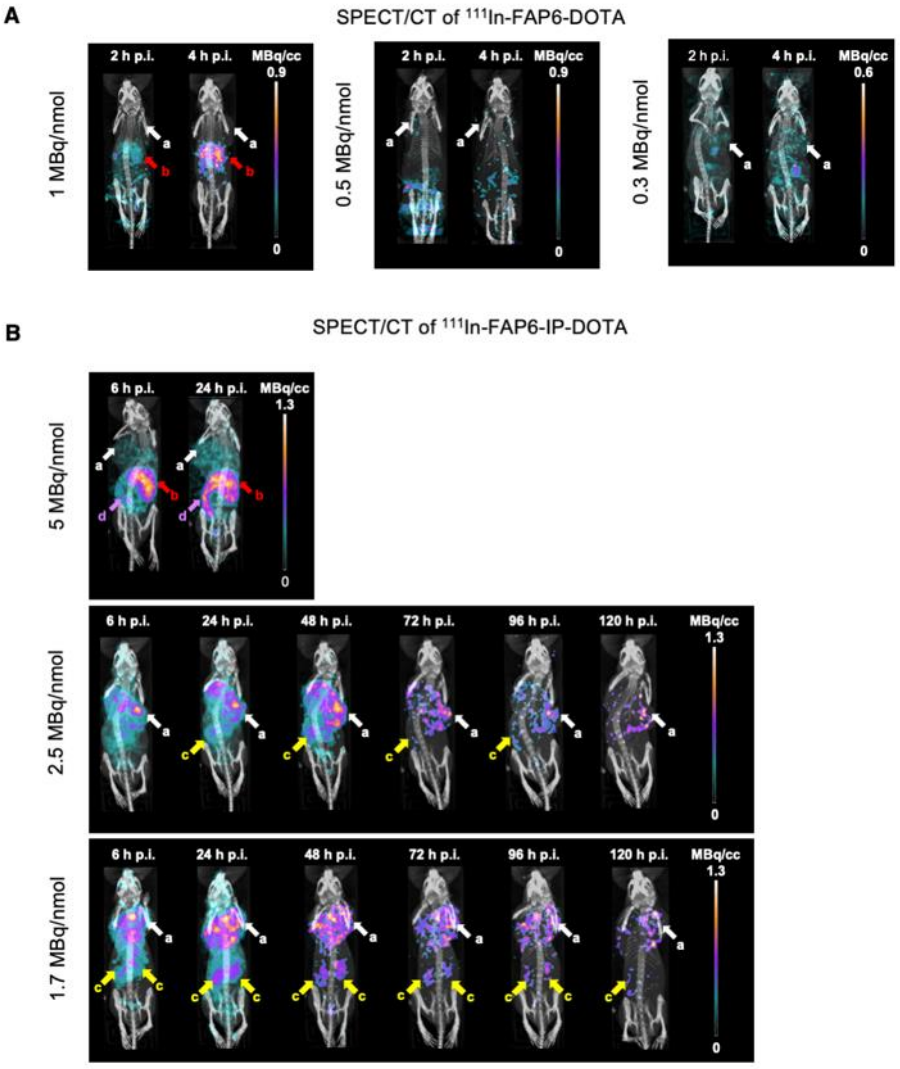

SUPPLEMENTAL FIGURE 6. Optimization of the specific activities of (**A**) ^{111}In-FAP6-DOTA and (**B**) ^{111}In-FAP6-IP-DOTA conjugates in 4T1 tumors over time as a function of molar amount of FAP6 conjugate injected while maintaining the dose of radioactivity constant (~10 MBq). Arrows: a = 4T1 tumors; b = liver; c = kidneys; d = spleen.

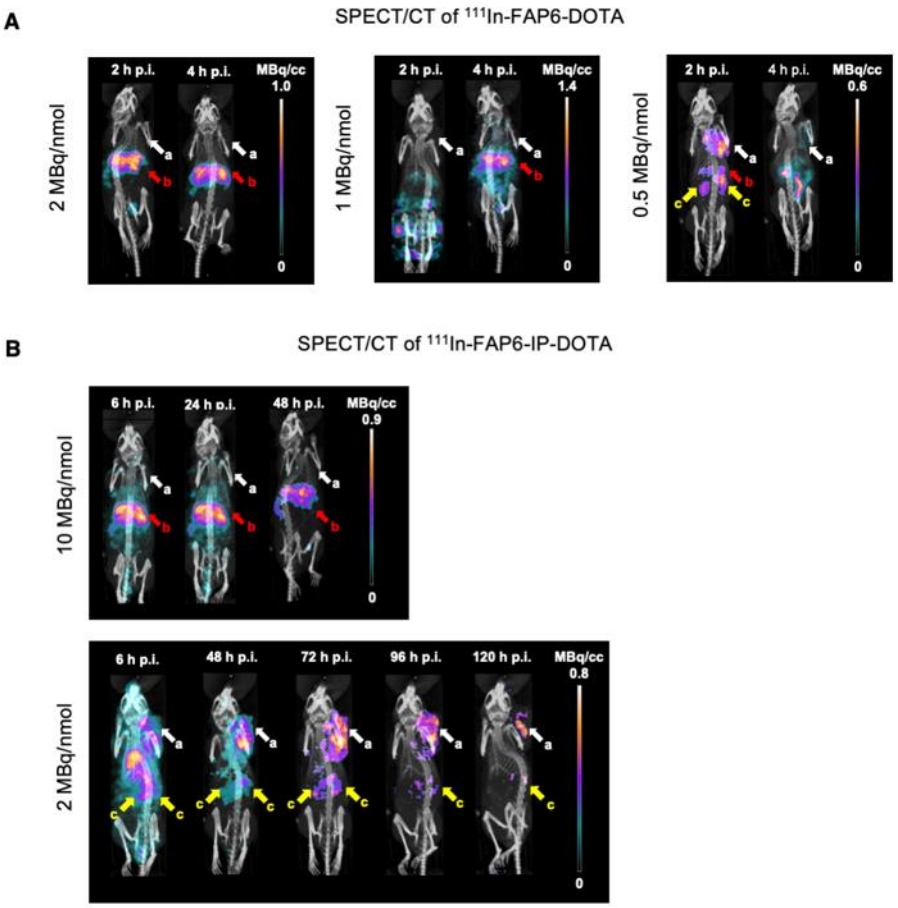

SUPPLEMENTAL FIGURE 7. Optimization of the specific activities of (**A**) ^{111}In-FAP6-DOTA and (**B**) ^{111}In-FAP6-IP-DOTA in HT29 tumors over time as a function of molar amount of FAP6 conjugate injected while maintaining the dose of radioactivity constant (~10 MBq). Arrows: a = 4T1 tumors; b = liver; c = kidneys.

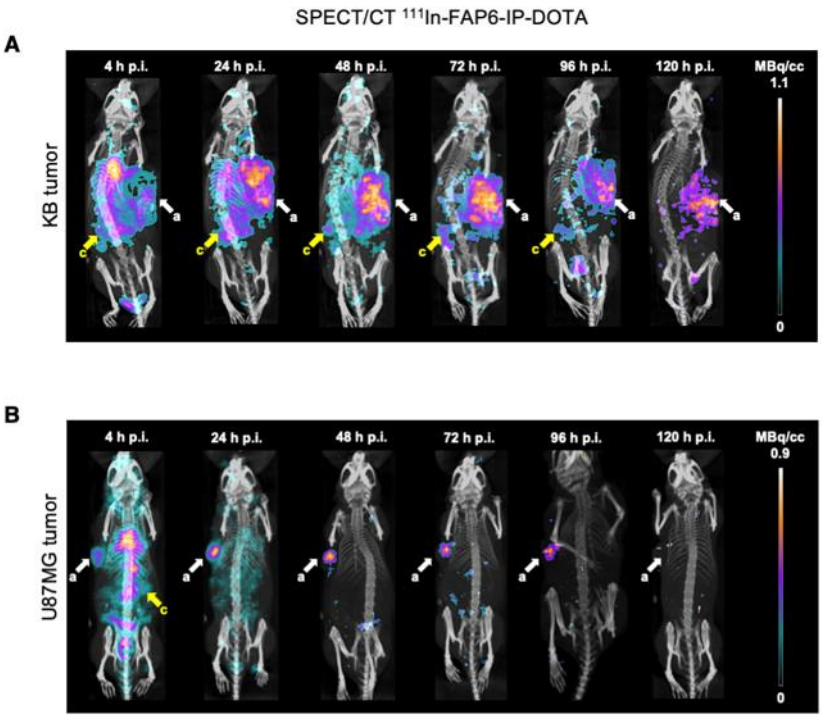

SUPPLEMENTAL FIGURE 8. Retention of ^{111}In-FAP6-IP-DOTA in (**A**) KB and (**B**) U87MG tumors as a function of time after injection. a: 4T1 tumors; b: liver; c: kidneys.

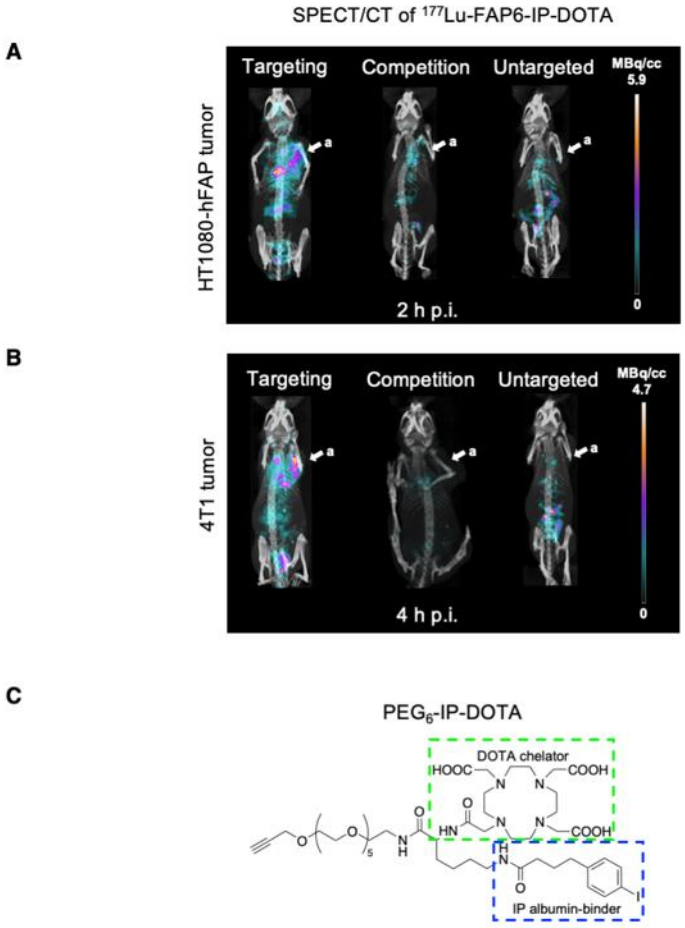

SUPPLEMENTAL FIGURE 9. Specificity studies of FAP6-IP-DOTA were conducted with ^{111}In-FAP6-IP-DOTA alone (targeting), ^{111}In-FAP6-IP-DOTA + 100x excess of cold compound (competition), or ^{111}In-PEG$_6$-IP-DOTA (untargeted). SPECT/CT scans were performed under all 3 conditions in (**A**) HT1080-hFAP and (**B**) 4T1 tumors. a: Tumors; b: liver; c: kidneys. (**C**) The molecular structure of PEG$_6$-IP-DOTA is provided, which was synthesized, radiolabeled, and evaluated in a manner analogous to FAP6-IP-DOTA.

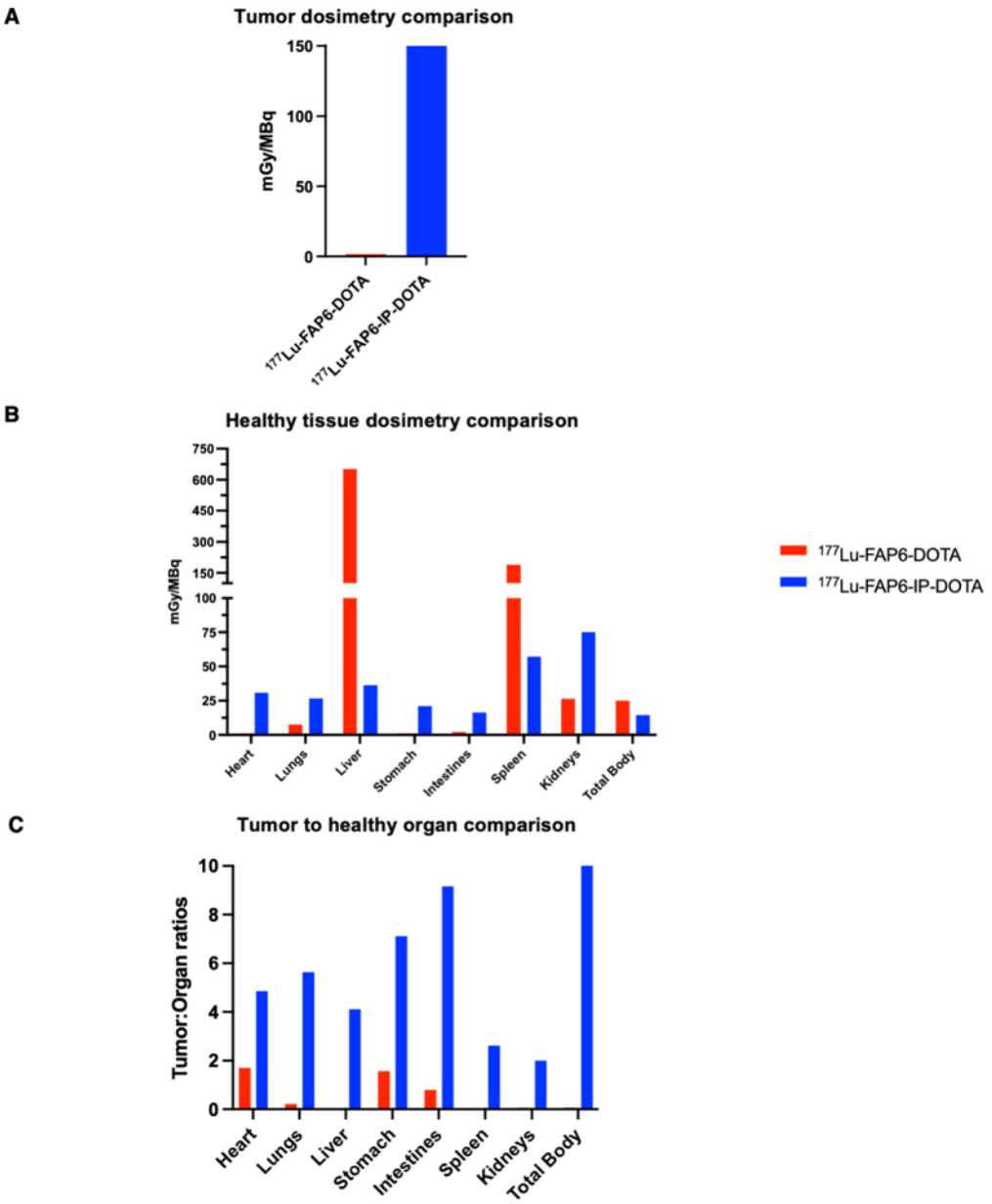

SUPPLEMENTAL FIGURE 10. Comparison of radiation dose estimates (mGy/MBq) delivered by ^{177}Lu-FAP6-DOTA (red bars) and ^{177}Lu-FAP6-IP-DOTA (blue bars) to (**A**) 4T1 tumors and (**B**) healthy organs as calculated by OLINDA 2.2.3. (**C**) Tumor to healthy organ ratios based on the calculated dosimetries in panels A and B are also provided.

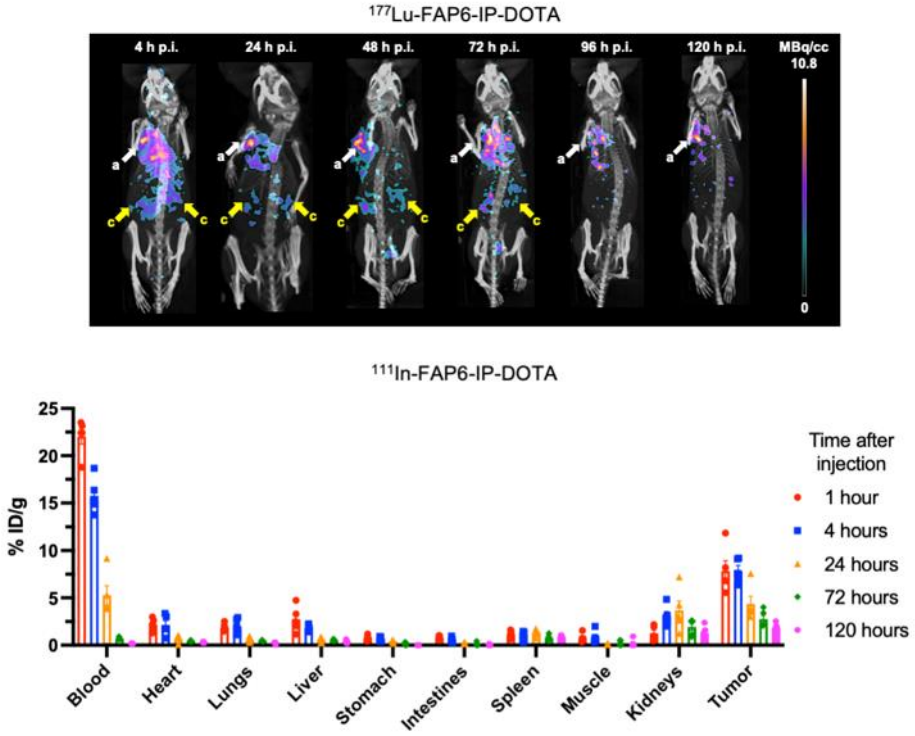

SUPPLEMENTAL FIGURE 11. SPECT/CT scans of ^{177}Lu-FAP6-IP-DOTA and biodistribution analysis of ^{111}In-FAP6-IP-DOTA in 4T1 tumor-bearing mice as a function of time after injection.

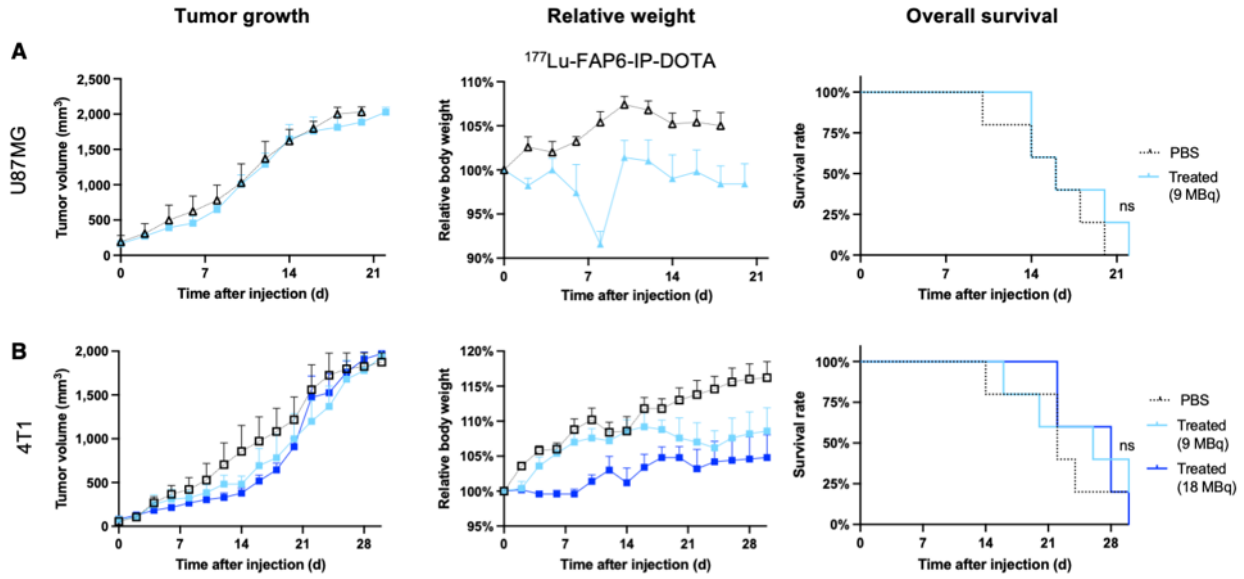

SUPPLEMENTAL FIGURE 12. Radioactive doses of ^{177}Lu-FAP6-IP-DOTA that were not effective for different tumor models are reported here. Briefly, mice bearing (**A**) U87MG (n = 5/group) or (**B**) 4T1 (n = 5/group) tumors received a single injection of ^{177}Lu-FAP6-IP-DOTA radiolabeled with the indicated amount of activity on day 0.

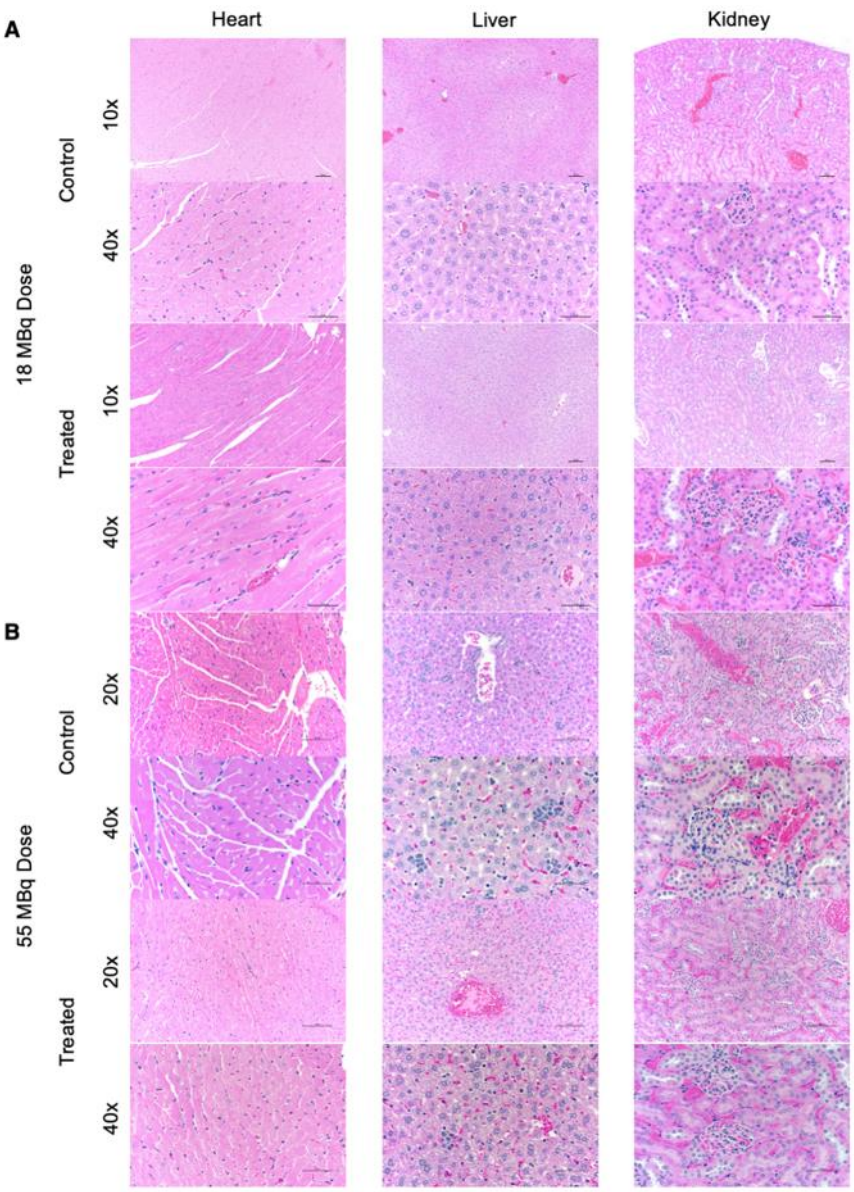

SUPPLEMENTAL FIGURE 13. Representative photomicrographs of 4 μm sections of mouse heart, liver, and kidney tissue following radiotherapy treatments of a single dose of ^{177}Lu-FAP6-IP-DOTA from Figures 5 and 6 [(**A**) 18 MBq in athymic nu/nu mice and (**B**) 55 MBq in Balb/c mice] stained with H&E.

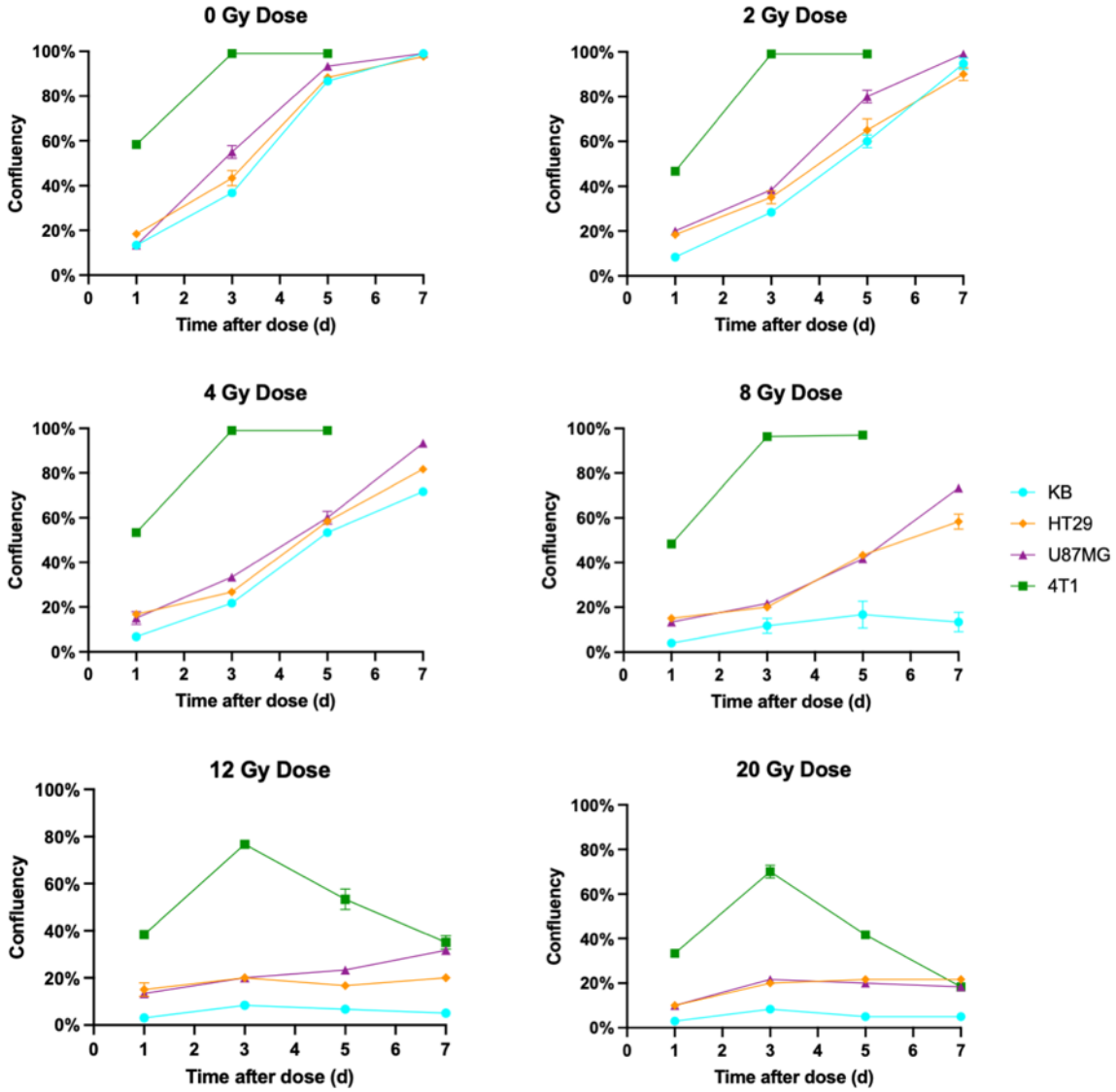

SUPPLEMENTAL FIGURE 14. The relative radiosensitivities of KB (●), HT29 (♦), U87MG (▲), and 4T1 (■) tumor cell lines were assessed by irradiation with an external beam at the indicated doses, followed by evaluation of the confluency of the cells every other day.

SUPPLEMENTAL TABLE 1. Biodistribution results of ^{177}Lu-FAP6-DOTA, ^{177}Lu-FAP6-IP-DOTA, and ^{111}In-FAP6-IP-DOTA in 4T1 tumors.

Organs	^{177}Lu-FAP6-DOTA in 4T1 tumors %ID/g mean ± SE				
	1 hours p.i.	4 hours p.i.	24 hours p.i.	72 hours p.i.	120 hours p.i.
Blood	0.45 ± 0.10	0.64 ± 0.41	0.01 ± 0.00	0.01 ± 0.00	0.01 ± 0.00
Heart	0.13 ± 0.01	0.04 ± 0.01	0.02 ± 0.00	0.05 ± 0.03	0.01 ± 0.00
Lungs	0.38 ± 0.04	0.09 ± 0.02	0.07 ± 0.03	0.04 ± 0.01	0.02 ± 0.01
Liver	8.99 ± 2.57	3.74 ± 2.11	6.32 ± 3.00	7.73% ± 3.02	5.19 ± 1.70
Stomach	0.02 ± 0.00	0.08 ± 0.03	0.04 ± 0.03	0.01 ± 0.00	0.01 ± 0.00
Intestines	0.14 ± 0.07	0.17 ± 0.13	0.01 ± 0.00	0.00 ± 0.00	0.00 ± 0.00
Spleen	2.62 ± 1.17	1.00 ± 0.45	1.80 ± 1.03	2.92 ± 0.83	1.90 ± 0.41
Muscle	0.02 ± 0.01	0.11 ± 0.03	0.02 ± 0.01	0.00 ± 0.00	0.00 ± 0.00
Kidneys	0.68 ± 0.16	0.53 ± 0.18	0.31 ± 0.09	0.24 ± 0.08	0.42 ± 0.11
Tumor	0.09 ± 0.05	0.09 ± 0.03	0.03 ± 0.01	0.01 ± 0.01	0.02 ± 0.01
	^{177}Lu-FAP6-IP-DOTA in 4T1 tumors %ID/g mean ± SE				
Blood	50.95 ± 3.97	28.13 ± 2.85	1.82 ± 0.10	0.19 ± 0.02	0.08 ± 0.00
Heart	2.14 ± 0.46	1.56 ± 0.19	0.41 ± 0.06	0.07 ± 0.04	0.05 ± 0.01
Lungs	2.12 ± 0.62	0.83 ± 0.21	0.71 ± 0.07	0.08 ± 0.01	0.06 ± 0.00
Liver	4.43 ± 0.27	1.17 ± 0.26	0.61 ± 0.08	0.13 ± 0.00	0.09 ± 0.01
Stomach	1.81 ± 0.27	0.88 ± 0.23	0.32 ± 0.06	0.04 ± 0.01	0.04 ± 0.01
Intestines	0.94 ± 0.15	0.71 ± 0.24	0.22 ± 0.03	0.05 ± 0.01	0.03 ± 0.00
Spleen	3.21 ± 0.25	2.55 ± 0.11	0.91 ± 0.15	0.32 ± 0.06	0.19 ± 0.01
Muscle	0.78 ± 0.17	0.73 ± 0.16	0.15 ± 0.02	0.04 ± 0.01	0.04 ± 0.01
Kidneys	2.77 ± 0.60	2.18 ± 0.58	0.88 ± 0.19	0.65 ± 0.15	0.46 ± 0.04
Tumor	12.15 ± 1.61	11.10 ± 1.89	2.16 ± 0.29	1.05 ± 0.24	0.54 ± 0.04
	^{111}In-FAP6-IP-DOTA in 4T1 tumors %ID/g mean ± SE				
Blood	22.06 ± 0.84	15.77 ± 0.84	5.28 ± 1.01	0.70 ± 0.05	0.18 ± 0.01
Heart	2.19 ± 0.30	2.12 ± 0.48	0.62 ± 0.21	0.44 ± 0.02	0.31 ± 0.03
Lungs	1.87 ± 0.19	2.00 ± 0.37	0.56 ± 0.13	0.46 ± 0.02	0.23 ± 0.05
Liver	2.73 ± 0.61	1.82 ± 0.15	0.55 ± 0.13	0.54 ± 0.03	0.41 ± 0.07
Stomach	0.77 ± 0.12	0.65 ± 0.11	0.40 ± 0.06	0.15 ± 0.06	0.01 ± 0.01
Intestines	0.80 ± 0.10	0.56 ± 0.11	0.23 ± 0.04	0.12 ± 0.08	0.03 ± 0.03
Spleen	1.20 ± 0.18	1.04 ± 0.20	1.33 ± 0.18	0.79 ± 0.13	0.85 ± .0.08
Muscle	0.77 ± 0.21	0.85 ± 0.29	0.13 ± 0.02	0.25 ± 0.11	0.20 ± 0.18
Kidneys	1.26 ± 0.31	3.07 ± 0.49	3.68 ± 1.01	1.93 ± 0.38	1.31 ± 0.33
Tumor	7.85 ± 1.08	7.86 ± 0.57	4.36 ± 0.81	2.77 ± 0.40	1.87 ± 0.22

SUPPLEMENTAL TABLE 2. Summarized histopathology of necropsy tissues post treatment.

Dose	Group	Organ	Total sections examined						Diagnostic lesions					
18 MBq	Control (n = 2)	Liver	8						0					
		Kidneys	16						0					
		Myocardium	8						0					
	Treated (n = 7)	Liver	38						0					
		Kidneys	56						0					
		Myocardium	28						0					
			Time after injection (d)						Time after injection (d)					
			1	3	7	14	21	Total	1	3	7	14	21	Total
55 MBq	Control (n = 5)	Liver	2	1	1	1	1	7	0	0	1	1	1	3
		Kidneys	4	4	4	4	4	20	0	0	0	0	0	0
		Myocardium	2	2	2	2	2	10	1	0	1	1	0	3
	Treated (n = 15)	Liver	5	3	3	3	3	17	0	0	0	0	2	2
		Kidneys	12	12	12	12	12	60	0	2	0	0	0	2
		Myocardium	6	6	6	6	6	30	0	0	0	0	1	1

References

1. Qian J, Olbrecht S, Boeckx B, et al. A pan-cancer blueprint of the heterogeneous tumor microenvironment revealed by single-cell profiling. *Cell Res.* 2020;30:745-762.

2. SCope tutorial: Pan-cancer TME blueprint. August 3, 2021; http://scope.lambrechtslab.org/#/a0f9b96f-e2d9-4156-9899-993e37a62c03/Breast.loom/tutorial. Accessed February 15, 2022.

3. Mukkamala R, Lindeman SD, Kragness KA, et al. Design and characterization of fibroblast activation protein targeted pan-cancer imaging agent for fluorescence-guided surgery of solid tumors. *J Mater Chem B.* 2022;10:2038-2046.

4. Tsai T-Y, Yeh T-K, Chen X, et al. Substituted 4-carboxymethylpyroglutamic acid diamides as potent and selective inhibitors of fibroblast activation protein. *J Med Chem.* 2010;53:6572-6583.